Rare Metal Materials and Engineering
Volume 46, Issue 8, August 2017
Online English edition of the Chinese language journal

Available online at www.sciencedirect.com
ScienceDirect

Cite this article as: Rare Metal Materials and Engineering, 2017, 46(8): 2049-2054.

ARTICLE

Influence of ZrO_2/Al_2O_3 Ratio in Carrier on Performance of Pt/ZrO_2-Al_2O_3 Catalyst

Yang Chaoqin[1], Wang Yaming[1], Wu Legang[2]

[1] Kunming University of Science and Technology, Kunming 650500, China; [2] Kunming Sino-Platinum Metals Catalyst Co., Ltd, Kunming 650221, China

Abstract: Diesel engines have been more and more widely used in heavy duty vehicles because of high efficiency and low fuel consumption compared with petrol engines. Taking ZrO_2 as the additive, the influence of the mass ratio of ZrO_2 to Al_2O_3 on catalytic performance was studied. The results show that, with an increase of ZrO_2 doping, the Pt particles become smaller at first and then larger in the catalyst. The interaction between Pt and the carrier increases, and then decreases. Analysis of the activity data shows the optimized doping amount of ZrO_2 is 40 wt% the complete oxidation temperatures of CO and C_3H_6 are reduced by 20 and 25 ^oC, respectively. When the ZrO_2/Al_2O_3 mass ratio in the carrier is varied, the precious metal dispersion on the catalyst and the precious metals interaction with the carrier are different with varying levels. The smaller the Pt particle size, the stronger the interaction between precious metal and the carrier, and the performance of catalyst is improved.

Key words: diesel vehicle; ZrO_2; catalyst; specific surface area; activity evaluation

According to a German Environmental Protection Bureau's survey, diesel engine exhausts pollutants of particulates and NO_x accounts for nearly half of all car emissions[1]. Nitrogen oxides, as a major air pollutant, are harmful to human health due to the formation of photochemical smog, acid rain, ozone depletion and greenhouse effect[2,3]. Several attempts are being implemented to reduce NO_x emissions, and one of the leading techniques is selective catalytic reduction by ammonia (NH_3-SCR), which has been extensively studied for lean NO_x control in stationary applications and diesel vehicle emissions[4-6]. In recent years, diesel engines have been more and more widely used in heavy duty vehicles because of their high efficiency and low fuel consumption compared with petrol engines. However, the particulate matter (PM) emissions, which cause environmental pollution and adverse health effects, are major a drawback of diesel engines[7-9]. To reduce PM emissions and protect human health, emission standards and legislations levels have been established in Europe, which demand after-treatment of the exhaust gases[10,11]. Important research has been completed in order to develop a suitable soot removal system for diesel vehicles[12,13]. Initially, diesel oxidation catalysts (DOC) technology was based on the use of Pt loaded on an alumina support. As emissions regulations became more stringent, however, both oxidation activity towards the PM and soluble organic fraction (SOF) at low temperatures and reduced oxidation of SO_2 became necessary aspects of DOC technology, and cerium-based catalysts which enabled the low temperature oxidation of the SOF became common, along with composite supports made from materials such as ZrO_2, because these substances exhibit low SO_2 adsorption. In addition, DOCs incorporating molecular sieves were developed, to improve the oxidation of THC, CO and the SOF under cold start conditions[14].

However, catalysts often show poor thermal stability under high-temperature conditions, which leads to severe catalytic deactivation and decreases the selectivity to CO_2 produced during the soot oxidation process[15,16]. One solution is to develop efficient and thermally stable catalysts[17,18]. It has been proved that the contact between the catalyst and soot markedly influences the reaction kinetics[17]. The most

Received date: September 14, 2016
Foundation item: National New Product (2011EG115008)
Corresponding author: Wang Yaming, Ph. D., Professor, Faculty of Chemical Engineering, Kunming University of Science and Technology, Kunming 650500, P. R. China, Tel/Fax: 0086-871-65920242, E-mail: wym@kmust.edu.cn

commonly used mixed oxides is ceria-zirconia ($Ce_xZr_{1-x}O_2$). Cerium is replaced with Zirconium in the crystal lattice. Zirconium doping also confers thermal stability to ceria. The importance of these mixed oxides catalysts has been raised in several studies for application to oxidation reactions[19-22]. Diverse oxide supports, such as ZrO_2, TiO_2, SiO_2, Al_2O_3 and CeO_2, have been reported to be useful in diesel soot oxidation catalysts. ZrO_2 that presents appropriate acid-base and redox properties is mentioned as a material that is moderately active to soot combustion[23-25]. Since ZrO_2 is an stable high- temperature material and can be used as the carrier of hydrocarbon compounds for catalytic combustion, it improves the interaction between the carrier and precious metal. Recently, adding a prescribed amount of ZrO_2 in Pd/Al_2O_3 systems to increase the reactivity and high-temperature stability of the system has been given extensive close attention[26].

In this study, ZrO_2 doped catalysts of different composition have been prepared by different methods, and soot combustion experiments have been performed with soot and catalyst solid particles mixed in the so-called "loose contact" mode[27]. The interaction of ZrO_2-Al_2O_3 has been widely studied in Pt catalysts; however, the research of ZrO_2-Al_2O_3 Pt catalysts are rare. Therefore, it is necessary to further study ZrO_2-Al_2O_3 systems in Pt catalysts.

In recent years, ZrO_2 based catalysts for selective catalytic reduction of NO_x with NH_3 were studied, and the precious metal catalysts were calcined in an electric furnace in air. Evaluations of the catalyst efficiency for oxidation performance for the species CO and C_3H_6 were carried out using a Simulated Gas Bench (SGB). Due to the difference of the ZrO_2-Al_2O_3 mass ratio in the carrier, specific surface area, crystal phase, and noble metal dispersion, REDOX properties of catalysts are distinct. In order to optimize the activity catalyst of CO and HC, characterizations such as BET, XRD, TPR, HRTEM were studied in detail.

1 Experiment

1.1 Preparation of the catalysts

A series of catalysts with different ZrO_2 doping (0, 20, 40, 60, 80, 100, wt%) were prepared by co-precipitation. Then they were impregnated with precious metals. The carrier was achieved by co-precipitation. Firstly, to obtain the required mixture of aluminum, and zirconium, a specific amount of Zirconium di-nitrate oxide ($Zr(NO_3)_2$) powder and white crystal aluminum nitrate ($Al(NO_3)_3$) were dissolved in deionized water and then mixed with a buffer solution consisting of $NH_3 \cdot H_2O$. After sediment deposition, mixing for 4 h, and then standing for 12 h, the mixture was dissolved in deionized water. The pH was controlled at around 9.0. The precipitates obtained were filtered and dried at 120 °C for 12 h. The precursor was placed in an oven for drying, then calcined for 4 h at 750 °C in a muffle furnace, and the composite oxide was identified as ZA. By adjusting the adding quantity of zirconium di-nitrate oxide and aluminum nitrate in the process of synthesis, the mass ratio of ZrO_2 and Al_2O_3 of composite oxide were varied from 0:100, 20:80, 40:60, 60:40, 80:20 to 100:0, and they were identified as ZA0, ZA20, ZA40, ZA60, ZA80 and ZA100, respectively.

Catalysts were obtained by the saturated impregnation method. A precious metal Pt solution with certain concentration was prepared, then the synthesized ZrO_2-Al_2O_3 composite oxide was added to the solution, and after stirring for a period of time, standing until being completely adsorbed, then calcined in air at 550 °C for 2 h in a oven, so the platinum compounds we selected will be pyrolysis into Pt^0/Pt^{2+}, and can be reduced under the emission reaction status. These samples with different ZrO_2 doping (wt%) of 0, 20, 40, 60, 80, 100 were labeled as PZA0 or (1), PZA20 or (2), PZA40 or (3), PZA60 or (4), PZA80 or (5), PZA100 or (6), respectively. Content of Pt was 1.5 wt% in all catalysts.

1.2 Catalytic activity measurement

Catalytic activity measurement was carried out by a 50 mm long quartz tubular fixed reactor bed by tabletting and sieving. 0.3 g of catalyst particles (420~250 μm) was used. The gas was made up of 1% CO and 5% O_2 for CO reaction, and N_2 was used as the equilibrium gas; the gas was made up of 0.3% C_3H_6 and 5% O_2 for C_3H_6 reaction, and N_2 was also used as the equilibrium gas. The space velocity of both model reaction was approximately 18000 mL $\cdot h^{-1} \cdot g^{-1}$. The type 7890 Agilent gas chromatograph was used for online analysis.

Temperature programmed reductions with H_2 (H_2-TPR) were carried out in a CHEMBET 3000 device, consisting of a tubular quartz reactor coupled to a thermal conductivity detector (TCD). Firstly, the sample was pretreated in Ar (80 mL $\cdot min^{-1}$) from room temperature (RT) to 120 °C, and held for 0.5 h. After cooling to room temperature (RT), and the samples were treated in H_2/Ar (80 mL $\cdot min^{-1}$) until TCD signal stabilized, and then heated to 800 °C with a rate of 10 °C /min.

The X-ray diffraction (XRD) experiments were performed on a Japan Science D/Max-R diffractometer using Cu Kα radiation (λ=0.154 06 nm), operated at 40 kV and 40 mA. The X-ray diffractogram was recorded at 0.01° intervals in the range of $10^o \le 2\theta \le 80^o$ with 3 s count accumulation per step. The identification of the phase was made with the help of JCPDS cards (Joint Committee on Powder Diffraction Standards).

Firstly, the sample was pretreated in H_2/Ar (80 mL $\cdot min^{-1}$) from RT to 450 °C, and held for 2 h. After the sample was pretreated in pure Ar (80 mL $\cdot min^{-1}$) to get a stable TCD signal baseline, the temperature was raised to 460 °C and kept for 10 min. After cooling to 80 °C and held for 0.5 h, the sample was titrated by pure CO (300 μL) until peak area kept constantly, and the peak area was recorded.

Ultrastructure and particle size of Pt in catalyst were observed by transmission electron microscopy (JEM-2100). The accelerating voltage was 200 KV. Firstly, the sample was

grinded, and then was dispersed by ultrasonic vibration with ethanol as dispersant. Finally, the sample was moved to observe in copper gauze.

2 Results and Discussion

2.1 Catalysts characterizations

N_2 adsorption-desorption isothermal curves of the catalysts with different aluminum zirconium doping are shown in Fig.1. The diagram shows the isotherms of PZA0 and PZA20 have obvious hysteresis when relative pressure P/P_0 between 0.4 and 1, which indicates the catalyst exhibits mesoporous structure. According to the classification of IUPAC[28], isotherm with hysteresis loops belongs to H_2 type. The visual characteristic of the porous of catalyst is worm shape. Fig.1 shows that, when the content of ZrO_2 is more than 20%, N_2 adsorption-stripping isotherms of catalysts are between I isotherm and IV isotherm, particularly PZA40 conforming to IV type isotherm. With the increase of ZrO_2 content, PZA100 conforms to I type isotherms. It shows that, with the increase of ZrO_2, the microporous structure of the catalysts increases gradually. The pore diameter distribution curves of the catalysts are shown in Fig.2. The diagram show pore diameter distribution of PZA0 and PZA20 have regular mesoporous hole peaks. With the increase of ZrO_2 content in the samples, the regularity of mesoporous structure weakens gradually, disappearing gradually from PZA40 to PZA100. However, microspore structure of the catalysts increases gradually. It conforms to the adsorption-stripping curves of the catalysts. The specific surface area, pore diameter and pore volume of the catalysts are listed in Table 1. In addition, compared to the commercial Al_2O_3, specific surface area of zirconium aluminum composite oxide is generally much larger except PZA80 and PZA100. When the carrier additive and the proportion of carrier are different, by different synthesis methods, they inevitably affect the interaction of precious metals with carrier of the catalysts, so as to influence the size of the precious metal particles.

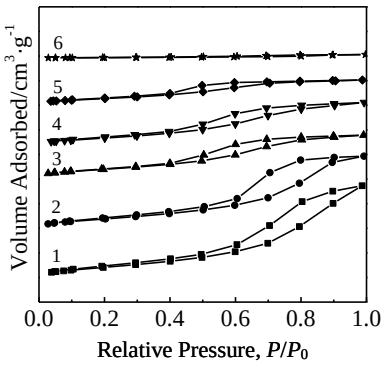

Fig. 1 N_2 isotherms of different catalysts (1-PZA0, 2-PZA20, 3-PZA40, 4-PZA60, 5-PZA80 and 6-PZA100)

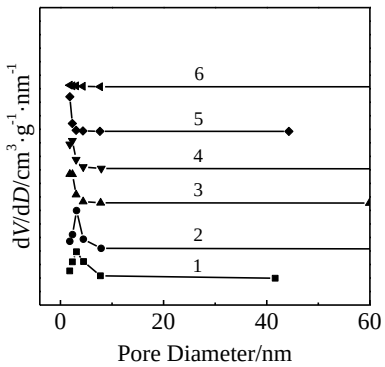

Fig.2 Pore size distribution of different catalysts (1-PZA0, 2-PZA20, 3-P ZA40, 4-PZA60, 5-PZA80 and 6-PZA100)

2.2 XRD results

XRD patters of different catalysts are shown in Fig.3. PZA0 only exhibits a peak for Al_2O_3, without the peak of any element or precious metal oxide. It shows that the precious metal is highly fragmented or forms tiny nano clusters (<5 nm). With the increase of the content of ZrO_2, a ZrO_2 morphology peak appear. However, PZA20 to PZA80 do not present any characteristic peak of elements or Pt oxide, which shows the Pt is highly fragmented. It is revealed that the interaction between Al_2O_3 and ZrO_2 can stabilize the ZrO_2 crystalline phases.

2.3 H_2-TPR results

The H_2-TPR spectra of different catalysts are shown in Fig.4. It is shown that the temperature for the reduction peak and peak area of PtO_x species is different in catalyst. The reducing peak temperature corresponds to the intensity of the interaction of species with the carrier. If the peak area is

Table 1 Physical properties and Pt dispersion of catalysts

Catalyst	$S_{(BET)}$/ $m^2\ g^{-1}$	Pore diameter/nm	Pore volume/ $cm^3\ g^{-1}$	Dispersion (Pt)/nm[29]
PZA0	235.1	3.1	0.6113	3.1
PZA20	215.0	3.1	0.4855	-
PZA40	180.2	2.2	0.3576	2.4
PZA60	170.2	< 2	0.2942	-
PZA80	123.9	< 2	0.1674	4.3
PZA100	7.7	< 2	0.0223	6.4

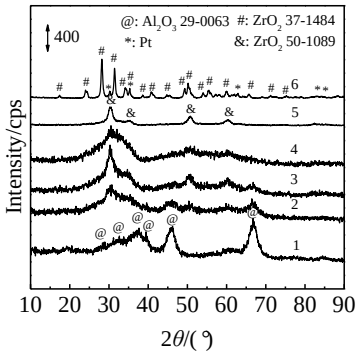

Fig.3 XRD patters of different catalysts (1-PZA0, 2-PZA20, 3-PZA40, 4-PZA60, 5-PZA80 and 6-PZA100)

different, the consumption is not the same as the amount of hydrogen, which is associated with the quantity of reduction species in catalyst. For Pt/Al_2O_3 samples, there are two reduction peaks: at 152 °C, which corresponds to the reduction of high dispersion of PtO; at 306 °C, which is in regard to the reduction of large particles. At the observed optimum doping level of ZrO_2, e.g. 40 wt%, the lower temperature for the reduction peak of catalyst is only 102 °C, while the high temperature reduction peak temperature is 290 °C. Compared with the unmodified sample, the temperature decreases by 50 °C and 16 °C, respectively. Compared with the H_2-TPR results of catalyst and catalyst performance on SGB for CO and C_3H_6, if reduction temperature of the species of PtO_x is lower, the peak area is greater, and thus the complete oxidation performance of CO and C_3H_6 is better.

2.4 HRTEM results

HRTEM results of different catalysts processed with different gas composition are shown in Fig.5. The figure shows for PZA0 loaded with pure Al_2O_3, the carrier exhibits a worm shape characteristic. This correlates to the Al_2O_3 carrier of catalyst; it is in line with the aforementioned specific surface area analysis. It is observed that the Pt particle size of PZA40 is minimum in the catalysts loaded with varying carrier additive proportions, while the Pt particles of PZA100 is the largest. It is consistent with XRD results.

2.5 In-situ infrared and pulse adsorption results

CO DRIFTS characterization technology and CO pulse adsorption technology were used for the complete qualitative and semi-quantitative analysis of precious metal particle size. The results are shown in Fig.6 and Table 1. The linear adsorption and the bridge type adsorption correspond to Pt particle size. The stronger the linear adsorption, the weaker bridge type adsorption, which shows that Pt particles are smaller, and vice versa. Fig.6 shows PZA40 has the highest linear adsorption intensity/bridge type adsorption intensity ratio, which indicates minimum Pt particle size. While PZA100 has the lowest linear adsorption intensity/bridge type adsorption intensity ratio, which illustrates larger Pt particles. It indicates that, the addition of ZrO_2 to modify the pure Al_2O_3 carrier enhances the interaction of precious metal Pt and

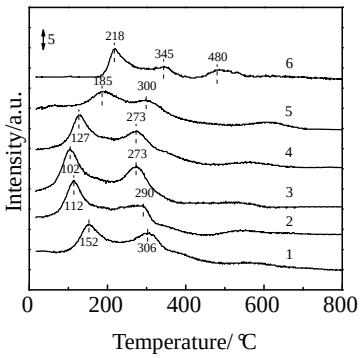

Fig.4 H_2-TPR spectra of different catalysts (1-PZA0, 2-PZA20, 3-PZA40, 4-PZA60, 5-PZA80 and 6-PZA100)

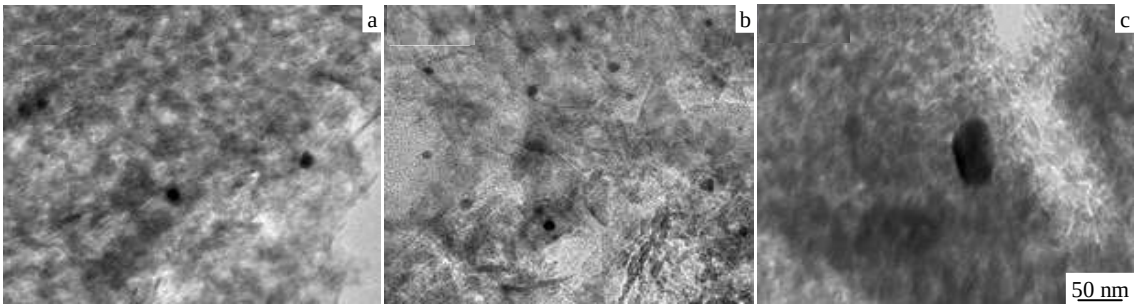

Fig.5 HRTEM for different catalysts: (a) PZA0, (b) PZA40, and (c) PZA100

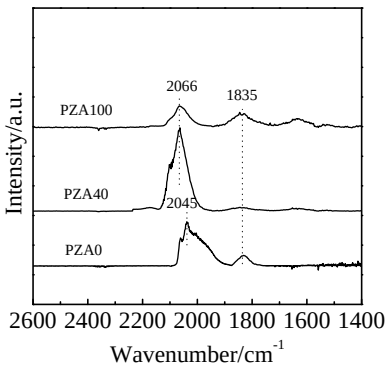

Fig.6 In-situ DRIFTS of CO of different catalysts

carrier (see H_2-TPR results), and promotes the precious metal Pt to disperse. While ZrO_2, when acting as the carrier, has low specific surface area of the carrier itself and poor interaction with the precious metal, and Pt particles increase sharply. XRD analysis can detect this interaction.

The results from CO pulse adsorption, HRTEM, CO Fourier in-situ infrared spectra and SGB for catalytic efficiency (CO and C_3H_6) were analyzed. Based on these analyses, the performance of catalyst is better when the precious metal Pt particles are smaller in the sample, and vice versa.

2.6 Catalytic activity evaluation results

Catalytic oxidation results of CO and C_3H_6 of different catalysts are shown in Fig.7 and Fig.8. The diagrams show

mass ratio of ZrO_2 and Al_2O_3 in the catalyst directly affects the catalytic activity. The complete oxidation temperatures for CO and C_3H_6 are 170 °C and 185 °C in PZA0, respectively. As the oxidation temperature of the selected species CO is low, and the relatively low temperature for C_3H_6 and for HC, but relatively high temperature for CO oxidation has the oxidation degree increases, which widens the sample to sample deviation of catalytic performance. Initially, adding ZrO_2 in the samples improved the performance of catalyst, especially in PZA40, and the complete oxidation temperatures of CO and C_3H_6 decrease to 150 and 160 °C, respectively. While complete oxidation temperature of CO and C_3H_6 reaches 200 and 215 °C in PZA100, respectively, compared with the performance of the optimal catalyst, where the complete oxidation temperature of CO and C_3H_6 increased by 50 and 55 °C, respectively. Through the analysis of results, it can be concluded that the optimal value for the doping amount of ZrO_2 is 40 wt%. Compared with the unmodified sample, the oxidation temperatures of CO and C_3H_6 are decreased by 20 and 25 °C, respectively.

In addition, it is unclear how long the life of doped PZA40 will be changed used aging catalyst and what construction the research in Zr with PZA40. Therefore, further demonstration will be carried out in our future work.

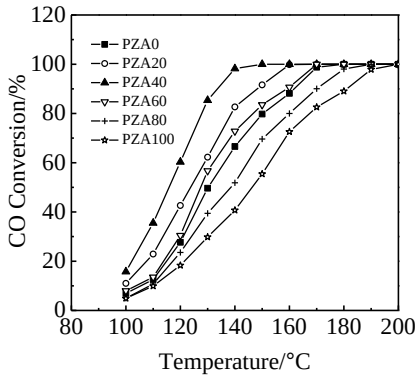

Fig.7 CO conversion curves for different catalysts

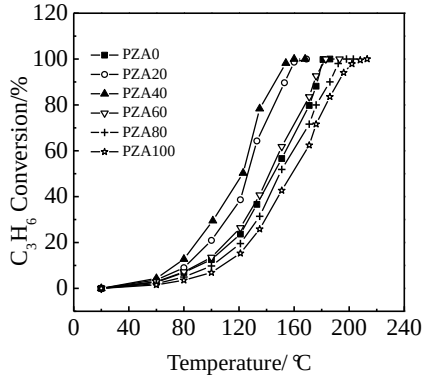

Fig.8 C_3H_6 conversion curves for different catalysts

As the carrier was loaded with Pt catalyst at different aluminum zirconium quality ratio, the specific surface area of the sample is gradually decreased as the ZrO_2 increases, and the Pt particle size of the samples and REDOX ability were decreased, and then increased. It shows that when noble metal particles are smaller, REDOX ability is stronger, and complete oxidation ability of the catalyst for CO and C_3H_6 is stronger.

3 Conclusions

1) The ZrO_2/Al_2O_3 mass ratio in the carrier is varied, and the precious metal dispersion on the catalyst and the precious metals interaction with the carrier are different. When precious metal dispersion degree is higher, the interaction is stronger, and the complete oxidation capability of the catalyst for CO and C_3H_6 is stronger, for catalyst with higher-performance is of higher specific surface area.

2) When the amount of ZrO_2 reaches an optimum of 40 wt%, the complete oxidation temperatures of CO and C_3H_6 decrease to 20 and 25 °C, respectively. Compared with the unmodified sample for CO and C_3H_6, catalytic oxidation performance is improved.

References

1 Walsh M P. *Platinum Metals Review*[J], 2000, 44(1): 22
2 Schultz M G, Diehl T, Brasseur G P *et al. Science*[J], 2003, 302(5645): 624
3 Skalska K, Miller J S, Ledakowicz S. *Science of the Total Environment*[J], 2010, 408(19): 3976
4 Nakajima F, Hamada I. *Catalysis Today*[J], 1996, 29(1): 109
5 Forzatti P. *Applied Catalysis A: General*[J], 2001, 222(1): 221
6 Liu Z, Ihl Woo S. *Catalysis Reviews*[J], 2006, 48(1): 43
7 Imran A, Varman M, Masjuki H *et al*. *Renewable and Sustainable Energy Reviews*[J], 2013, 26: 739
8 Wierzbicka A, Nilsson P T, Rissler J *et al. Atmospheric Environment*[J], 2014, 86: 212
9 Harrison P G, Ball I K, Daniell W *et al*. *Chemical Engineering Journal*[J], 2003, 95(1): 47
10 Pui D Y, Chen S C, Zuo Z. *Particuology*[J], 2014, 13: 1
11 Chhiti Y, Peyrot M, Salvador S. *Journal of Energy Chemistry*[J], 2013, 22(5): 701
12 Twigg M V. *Applied Catalysis B: Environmental*[J], 2007, 70(1): 2
13 Frank B, Schuster M E, Schlögl R *et al. Angewandte Chemie International Edition*[J], 2013, 52(10): 2673
14 Sampara C S, Bissett E J, Assanis D. *Chemical Engineering Science*[J], 2008, 63(21): 5179
15 Lin F, Wu X, Liu S *et al*. *Chemical Engineering Journal*[J], 2013, 226: 105
16 Wu X, Liu S, Weng D *et al. Journal of Hazardous Material*[J], 2011, 187(1-3): 283
17 Nejar N, Garcia C J, Lecea C *et al*. *Catalysis Communications*[J], 2005, 6(4): 263
18 Kureti S, Weisweiler W, Hizbullah K. *Applied Catalysis B:*

Environmental[J], 2003, 43(3): 281
19 Guillen-Hurtado N, Bueno-Lopez A, Garcia-Garcia A. *Applied Catalysis A-General*[J], 2012, 437: 166
20 Aneggi E, de Leitenburg C, Trovarelli A. *Catalysis Today*[J], 2012, 181(1): 108
21 Liu L, Yao Z, Liu B *et al*. *Journal of Catalysis*[J], 2010, 275(1): 45
22 Nelson A E, Schulz K H. *Applied Surface Science*[J], 2003, 210(3-4): 206
23 Liu J, Zhao Z, Xu C *et al*. *Applied Catalysis B: Environmental*[J], 2005, 61(1): 36
24 Galdeano N, Carrascull A, Ponzi M *et al*. *Thermochimica Acta*[J], 2004, 421(1): 117
25 Carrascull A, Grzona C, Lick D *et al*. *Reaction Kinetics and Catalysis Letters*[J], 2002, 75(1): 63
26 Van Setten B, Schouten J M, Makkee M *et al*. *Applied Catalysis B-Environmental*[J], 2000, 28(3-4): 253
27 Müller C A, Maciejewski M, Koeppel R A *et al*. *Catalysis Today*[J], 1999, 47(1): 245
28 Sing K S. *Pure and Applied Chemistry*[J], 1985, 57(4): 603
29 Avila M S, Vignatti C I, Apesteguía C R *et al*. *Catalysis Letters* [J], 2010, 134(1-2): 118

载体中 ZrO_2/Al_2O_3 比对 Pt/ZrO_2-Al_2O_3 催化剂性能的影响

阳超琴[1]，王亚明[1]，吴乐刚[2]
(1. 昆明理工大学，云南 昆明 650500)
(2. 昆明贵研催化有限公司，云南 昆明 650221)

摘 要：相比汽油车而言，柴油车具有高效、低油耗的优势已得到广泛应用。本实验以 ZrO_2 作为改性剂，探究了 ZrO_2 与 Al_2O_3 的质量比对催化剂的影响。结果表明：随着 ZrO_2 的加入，Pt 粒子先减小后增大；Pt 粒子与载体的交互作用先增大后减小。活性实验数据的分析表明，ZrO_2 的最佳添加质量分数为 40%，CO 和 C_3H_6 完全氧化温度分别降低 20 和 25 ℃。贵金属在催化剂的分散度以及贵金属与载体的相互作用随着 ZrO_2 与 Al_2O_3 质量比的变化而变化。Pt 粒子越小，其与载体的交互作用越强，这表明催化剂性能越强。

关键词：柴油车；ZrO_2；催化剂；比表面积；活性评价

作者简介：阳超琴，女，1971 年生，博士生，讲师，昆明理工大学化学工程学院，云南 昆明 650500，电话：0871-65920242，E-mail: kustycq@126.com